IIJP 2026 | Volume 2, Issue 1, pp. 1468-1484 | ISSN: 2636-4484

COMPARATIVE PERFORMANCE OF SENSIBLE AND LATENT THERMAL ENERGY STORAGE SYSTEMS FOR SOLAR ELECTRICITY IN NORTH-EASTERN NIGERIA

Wilfred Manliura Amthombata[1], Abubakar Alkasim[2] & Pascal Timtere[3]
[1] *Physics Department, Adamawa State College of Education, Hong, Nigeria*
manliurawilfred45@yahoo.com/+2347035886631
[2] *Physics Department, Modibbo Adama University, Yola, Nigeria*
alkasimabbat@mau.edu.ng/+2348180403135
[3] *Physics Department, Modibbo Adama University, Yola, Nigeria*
Email: timterepascal@mau.edu.ng/+2347039048370
Corresponding Author: *Wilfred, M. A. (manliurawilfred45@yahoo.com)*

ARTICLE INFO
Article No.: 0241
Accepted Date: 06/03/2026
Published Date: 30/03/2026
Type: Research

ABSTRACT
Thermal energy storage (TES) is an important technology for improving the dispatchability of solar-based electricity systems in regions with high solar potential but limited grid infrastructure. This study presents a unified dynamic simulation framework for the comparative evaluation of sensible and latent TES systems integrated into a 100 kW decentralized solar electricity generation configuration under the high-irradiance climatic conditions of North-Eastern Nigeria. A rock-bed sensible heat storage (SHS) system and three nitrate-based latent heat storage (LHS) materialsSolar Salt, sodium nitrate ($NaNO_3$), and potassium nitrate (KNO_3) was modeled using a consistent MATLAB/Simulink architecture incorporating region-specific solar irradiance and ambient temperature data. All storage systems were evaluated under identical operating conditions, boundary parameters, and solver settings to isolate intrinsic material-dependent performance. Results indicate a recoverable thermal energy of approximately 210 kWh per cycle for the rock-bed SHS system with a round-trip efficiency of 75–80%. In contrast, latent heat storage systems achieved significantly higher storage capacities: Solar Salt ≈ 1300 kWh, $NaNO_3$ ≈ 780 kWh, and KNO_3 ≈ 520 kWh per cycle. Solar Salt also demonstrated the most stable quasi-isothermal discharge behavior and the highest efficiency range (80–85%). Sensitivity analysis (±10% thermophysical variation and ±15% HTF flow rate) confirmed that comparative performance trends remain robust under realistic parameter uncertainty. Model validation against published experimental data showed efficiency deviations within ±5%. The results provide a climate-specific framework for TES material selection in decentralized solar electricity systems in arid regions.

Keywords: Thermal energy storage; Sensible heat storage; Latent heat storage; Phase change materials; Solar electricity; North-Eastern Nigeria

1. Introduction

Electricity access remains limited across many parts of sub-Saharan Africa, particularly in rural and conflict-affected regions. Nigeria experiences one of the largest electricity access deficits globally (World Bank, 2020). In North-Eastern Nigeria, electricity supply is further constrained by limited grid penetration, dispersed settlements, and fragile infrastructure. These conditions make the expansion of centralized power systems difficult and highlight the need for decentralized energy solutions capable of providing stable and dispatchable electricity.

North-Eastern Nigeria possesses substantial solar energy potential. Average daily global horizontal irradiance in the region ranges between approximately 5.5 and 6.5 kWh m^{-2} day^{-1} (European Commission Joint Research Centre [JRC], 2023; National Aeronautics and Space Administration [NASA], 2023). Although this resource supports solar-based electricity generation, the intermittent nature of solar radiation creates temporal mismatches between energy supply and demand. In off-grid and weak-grid environments, such variability can reduce system reliability unless effective energy storage technologies are incorporated.

Thermal energy storage (TES) has emerged as an important technology for improving the dispatchability of solar thermal and concentrated solar power (CSP) systems. By separating the timing of energy collection from electricity generation, TES enhances operational flexibility and reduces energy curtailment (International Energy Agency [IEA], 2023; International Renewable Energy Agency [IRENA], 2022). TES technologies are generally classified into two main categories: sensible heat storage (SHS), where energy is stored through temperature changes in a storage medium, and latent heat storage (LHS), where phase change materials (PCMs) absorb and release energy during phase transitions at nearly constant temperature.

Packed rock-bed systems are among the most widely investigated SHS configurations because of their structural simplicity, durability, and relatively low material cost. However, their energy density is limited because stored energy depends mainly on the specific heat capacity of the material and the temperature difference achieved during operation (Li *et al*., 2023; Peng *et al*., 2020). In contrast, latent heat storage systems provide higher volumetric energy density by utilizing the latent heat absorbed during phase transitions. This mechanism enables improved thermal buffering and more stable discharge behavior (Xu *et al*., 2020; Zhang *et al*., 2021). Previous experimental and numerical studies have also reported improved discharge uniformity and slightly higher round-trip efficiencies for nitrate-based PCMs compared with purely sensible heat storage systems (Prieto *et al.*, 2022).

Among high-temperature TES materials, inorganic nitrate salts such as sodium nitrate ($NaNO_3$), potassium nitrate (KNO_3), and their eutectic mixture known as Solar Salt have received significant attention. These materials possess favorable melting temperatures, good thermal stability, and compatibility with CSP operating conditions (Cabeza *et al*., 2021; Prieto *et al*., 2022). Solar Salt is already widely used in commercial CSP plants because of its stable thermophysical properties and relatively high latent heat capacity. However, the comparative performance of individual nitrate salts under identical operating conditions can vary depending on system configuration and operating constraints.

Despite extensive global research on TES technologies, many comparative modeling studies are based on climatic assumptions representative of temperate regions. These studies often employ moderate ambient temperatures and boundary conditions that differ substantially from those found in arid and semi-arid environments. In regions such as North-Eastern Nigeria, ambient temperatures frequently exceed 40 °C, and strong diurnal temperature variations influence thermal gradients within storage systems. High ambient temperatures can reduce the effective temperature difference between the storage medium and its surroundings, thereby influencing heat losses,

thermocline stability in sensible storage systems, and phase transition behavior in latent heat storage systems. Nevertheless, these climate-specific effects are rarely examined within comparative SHS–LHS simulation frameworks.

Furthermore, much of the existing TES literature focuses on utility-scale CSP installations with multi-megawatt thermal capacities. Comparatively little attention has been given to medium-scale decentralized systems, such as those designed for approximately 100 kW electrical output, which are more relevant for off-grid electrification. At this scale, system performance can be strongly influenced by storage volume limitations, daily charging cycles, and operational constraints that differ from those of large-scale power plants.

This study addresses these research gaps by developing a unified transient MATLAB/Simulink modeling framework for a rock-bed sensible heat storage system and three nitrate-based latent heat storage systems. The models incorporate region-specific solar irradiance and ambient temperature conditions representative of North-Eastern Nigeria. The framework is used to evaluate charging–discharging behavior, thermocline development, phase transition stability, and recoverable energy capacity. By focusing on a decentralized 100 kW solar electricity generation configuration and performing parametric sensitivity analysis, the study provides a context-specific comparative evaluation of sensible and latent TES technologies for off-grid solar energy applications.

2 Material and Method

2.1 Study Design

A simulation-based comparative framework was developed to evaluate the thermodynamic performance of sensible heat storage (SHS) and latent heat storage (LHS) systems integrated into a 100 kW solar electricity generation configuration representative of North-Eastern Nigeria. The modeling architecture was implemented in MATLAB/Simulink using a modular structure comprising solar input, heat exchange, storage, and power conversion subsystems. All storage configurations were subjected to identical boundary conditions, operating temperature ranges, and nominal electrical output constraints in order to isolate intrinsic material-dependent performance characteristics.

2.2 Solar Resource and Collector Model

Representative solar resource conditions were obtained from long-term satellite datasets for North-Eastern Nigeria (JRC, 2023; NASA, 2023). A baseline daily global horizontal irradiance of approximately 6.0 kWh m^{-2} day^{-1} was adopted to represent typical regional solar availability. A parabolic trough collector (PTC) was selected to convert incident solar radiation into thermal energy for the thermal energy storage (TES) system. PTC technology operates effectively within 150–400 °C, making it suitable for both rock-bed sensible heat storage and nitrate-based molten salt phase-change materials (Bellos & Tzivanidis, 2022; Ghosh *et al*., 2023).

The useful thermal power output from the collector is estimated using the solar thermal energy balance:

$$\dot{Q}_{solar} = GA_c\eta_c \quad (2.1)$$

where $\dot{Q}_{solar}$is the useful thermal power output (W), $G$is solar irradiance (W m^{-2}), A_c is the collector absorber area (m^2), and η_c is collector efficiency.

For the baseline configuration, collector efficiency was assumed to be 0.7, consistent with typical parabolic trough performance, while peak solar irradiance was taken as 1000 W m^{-2} based on regional satellite observations (NASA POWER, 2023; NiMet, 2024).

To supply the required 100 kW thermal input for TES charging, the collector area was determined as:

$$A_c = \frac{\dot{Q}_{solar}}{G\eta_c} \quad (2.2)$$

Substituting $\dot{Q}_{solar} = 100{,}000\text{W}$, $G = 1000\text{W m}^{-2}$, and $\eta_c = 0.7$ yields an absorber area of approximately 143 m².

The captured heat is transferred via a heat transfer fluid (HTF) loop to charge the TES units during daytime operation, while stored thermal energy is discharged through the power conversion subsystem during non-solar periods. System operation was simulated over a 24-hour cycle consisting of daytime charging and controlled nighttime discharge to maintain a nominal 100 kW electrical output. Collector efficiency was assumed constant, with optical and thermal losses implicitly represented within the efficiency parameter.

2.3 Thermal Energy Storage Configurations

Two thermal energy storage (TES) approaches were evaluated:

(i) Sensible heat storage (SHS): A packed rock-bed system in which energy is stored through temperature increase of a solid medium.

(ii) Latent heat storage (LHS): Phase change material (PCM) systems using Solar Salt, sodium nitrate ($NaNO_3$), and potassium nitrate (KNO_3), where energy storage occurs primarily through solid–liquid phase transition.

All systems were dimensioned to deliver a comparable nominal electrical output of 100 kW, enabling direct performance comparison.

2.4 Governing Energy Balance Relations

The transient behavior of the TES systems was modeled using first-principles energy conservation under cyclic charging and discharging conditions. Separate formulations were developed for sensible and latent storage systems to reflect their distinct thermodynamic mechanisms.

2.4.1 General Energy Balance

For a control volume representing the storage medium, the transient energy balance is expressed as:

$$\frac{dE_{st}}{dt} = \dot{Q}_{in} - \dot{Q}_{out} - \dot{Q}_{loss} \quad (2.3)$$

where E_{st} is the stored thermal energy (J), $\dot{Q}_{in}$ is the heat input rate (W), $\dot{Q}_{out}$ is the discharge heat rate (W), and $\dot{Q}_{loss}$ represents heat losses to the surroundings (W).

Because the storage tanks were assumed to be well insulated, external losses were considered negligible ($\dot{Q}_{loss} \approx 0$), reducing the balance to the difference between charging and discharging heat rates.

2.4.2 Rock-Bed Sensible Heat Storage Model

For the packed rock-bed system, thermal energy is stored through temperature variation of the solid medium. The stored energy is expressed as:

$$Q_{SHS} = m_r c_{p,r}(T_{max} - T_{min}) \quad (2.4)$$

where m_r is the rock mass (kg), $c_{p,r}$ is the specific heat capacity (J kg^{-1} K^{-1}), and T_{max} and T_{min} are the maximum and minimum operating temperatures.

The rock mass is obtained from:

$$m_r = \rho_r V_r \quad 2.5)$$

where ρ_r is rock density (kg m^{-3}) and V_r is the storage volume (m³).

This formulation reflects the sensible heat mechanism, in which stored energy varies linearly with temperature difference and heat capacity. Heat transfer was modeled as one-dimensional along the axial flow direction with uniform temperature distribution within each simulation step.

2.4.3 Phase Change Material Energy Storage Model

For latent heat storage systems, the total stored energy includes both sensible and latent components:

$$Q_{PCM} = m_p c_{p,s}(T_m - T_i) + m_p L + m_p c_{p,l}(T_f - T_m) \quad (2.6)$$

where m_p is the PCM mass (kg), $c_{p,s}$ and $c_{p,l}$ are specific heat capacities of the solid and liquid phases (J kg^{-1} K^{-1}), T_i is the initial temperature, T_m is the melting temperature, T_f is the final charging temperature, and L is the latent heat of fusion (J kg^{-1}). The latent term represents the energy absorbed during phase transition at nearly constant temperature, which contributes to the higher storage density of nitrate-based PCMs. Complete melting during charging and solidification during discharge were assumed for cyclic operation.

2.4.4 Turbine Power Equation

During discharge, stored thermal energy is converted to electricity using a simplified Rankine-cycle representation:

$$P_e = \dot{Q}_{dis}\, \eta_{turb}\, \eta_{gen} \quad (2.7)$$

where P_e is electrical power output (W), $\dot{Q}_{dis}$is the thermal discharge rate (W), η_{turb} is turbine efficiency, and η_{gen} is generator efficiency.

The combined conversion efficiency is:

$$\eta_{conv} = \eta_{turb} \times \eta_{gen} \quad (2.8)$$

Using $\eta_{turb} = 0.88$and $\eta_{gen} = 0.96$, the overall thermal-to-electric efficiency is approximately 84.5%. This simplified representation provides a computationally efficient approximation suitable for comparative TES performance analysis.

2.5 Storage Efficiency Metric

To evaluate storage performance independently of the power conversion block, the round-trip thermal efficiency is defined as:

$$\eta_{rt} = \frac{Q_{dis}}{Q_{ch}} \quad (2.9)$$

where Q_{ch} is the thermal energy supplied during charging and Q_{dis} is the useful energy recovered during discharge.

These metric captures storage-related losses such as heat-transfer limitations, thermocline dispersion in SHS systems, and incomplete phase transitions in LHS systems. Unless otherwise stated, efficiencies reported in the Results section refer to this round-trip thermal efficiency.

2.6 Simulation Parameters

Representative thermophysical properties and operating conditions used in the simulations are summarized in Table 1. Parameter values were selected from established TES and nitrate-salt literature to ensure consistency with reported performance ranges (Cabeza *et al*., 2021; Prieto *et al*., 2022).

Table 1

Key thermal energy storage simulation parameters

Parameter	SHS (Rock bed)	Solar Salt	$NaNO_3$	KNO_3
Storage volume (m^3)	9.2	10.0	4.78	3.41
Density (kg m^{-3})	2600	1800	1800	1800
Specific heat (J kg^{-1} K^{-1})	920	1500	1500	1500
Latent heat (kJ kg^{-1})	—	260	260	260
Operating temperature (°C)	250–400	220–350	220–330	220–330
Heat exchanger efficiency	0.90	0.90	0.90	0.90
Turbine efficiency	0.88	0.88	0.88	0.88
Generator efficiency	0.96	0.96	0.96	0.96

Note. Latent heat values are expressed in kJ kg^{-1} consistent with PCM literature.

2.7 Modeling Assumptions

Several simplifying assumptions were adopted to ensure consistent and computationally efficient comparative analysis. Heat transfer within the storage media was modeled as one-dimensional along the axial flow direction, while radial temperature gradients were neglected. External heat losses were assumed negligible due to effective insulation, allowing isolation of intrinsic storage behavior. The heat transfer fluid (HTF) was assumed perfectly mixed at the inlet and outlet manifolds, producing uniform temperatures at each simulation step. Thermophysical properties were considered temperature-independent within each phase region, with constant specific heat values for sensible storage and for the solid and liquid phases of the PCMs.

These assumptions are commonly used in TES modeling and provide a consistent baseline for comparative system-level performance evaluation rather than detailed multidimensional heat transfer analysis.

2.8 Temperature-Dependent Thermophysical Properties

Although baseline simulations assumed constant thermophysical properties, high-temperature storage materials exhibit moderate variation across the operating range (220–400 °C). For rock-based systems, specific heat capacity and thermal conductivity may vary by approximately 5–12% over a temperature interval of about 150 K, while nitrate-based PCMs exhibit temperature-dependent sensible heat capacities in both solid and liquid phases.

These variations can be approximated using linearized relations:

$$C_p(T) = C_{p,0} + aT \tag{2.10}$$

$$k(T) = k_0 + bT \tag{2.11}$$

where $C_p(T)$ is temperature-dependent specific heat capacity (J kg^{-1} K^{-1}), $C_{p,0}$is the reference value, $k(T)$is thermal conductivity (W m^{-1} K^{-1}), and $a$and $b$are empirical temperature coefficients. For nitrate PCMs, temperature dependence is applied separately to the solid and liquid phases, while latent heat absorption occurs at the melting temperature. A parametric sensitivity analysis (Section 3.7) confirmed that moderate property variation does not significantly alter comparative storage performance trends, supporting the constant-property assumption for system-level analysis.

2.9 Modular Simulink Architecture and Subsystem Interaction

A unified modular framework was developed in MATLAB/Simulink to ensure reproducibility and consistent comparison of sensible and latent thermal energy storage (TES) systems. The model consists of interconnected subsystems: (i) solar resource and thermal

collection module, (ii) heat transfer fluid (HTF) circulation unit, (iii) interchangeable TES subsystem, (iv) power conversion block, and (v) supervisory control unit. All configurations operate under identical numerical settings, boundary conditions, and solver parameters to maintain unbiased material comparison.

Figure 1 illustrates the subsystem architecture and energy flow during charging and discharge operation.

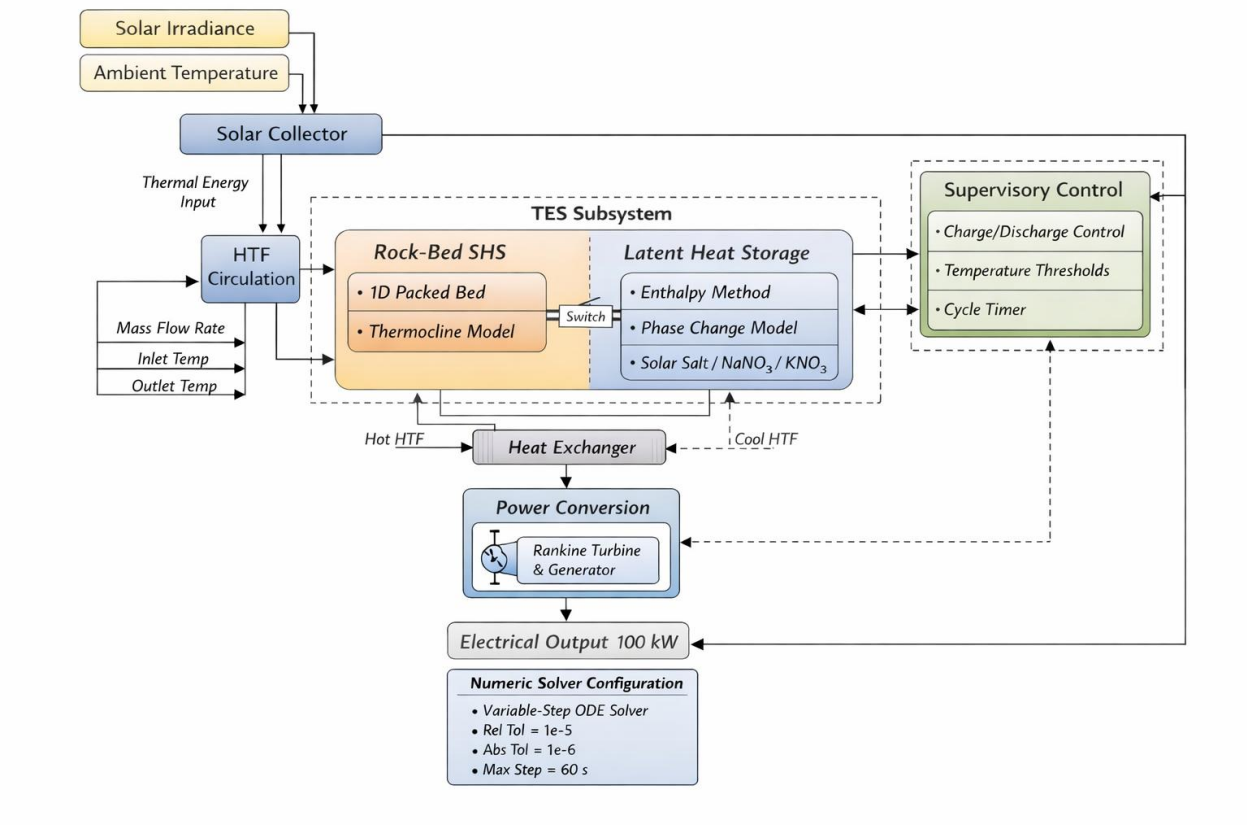

Figure 1

Modular MATLAB/Simulink architecture showing subsystem interconnections and bidirectional energy flow during charging and discharge modes.

The solar resource module incorporates region-specific irradiance and ambient temperature data representative of North-Eastern Nigeria. Instantaneous thermal gain from the solar collector is calculated as:

$$Q_{solar} = \eta_{collector} A_{collector} G(t) \tag{2.11}$$

where $G(t)$is the solar irradiance, $A_{collector}$is the collector aperture area, and $\eta_{collector}$is the collector efficiency. The resulting thermal energy is transferred through the HTF loop, which dynamically represents mass flow rate and temperature exchange between the collector and storage unit.

The TES subsystem is implemented as interchangeable modules within the same simulation framework:

(i) Rock-bed sensible heat storage (SHS): modeled using a one-dimensional packed-bed representation that captures thermocline development and axial temperature gradients.

(ii) Latent heat storage (LHS): modeled using an enthalpy-based phase-change formulation for Solar Salt, $NaNO_3$, and KNO_3, where phase transition is represented through an effective heat capacity approach.

Only one TES configuration is active in each simulation run, while all other subsystems remain unchanged, ensuring solver consistency and isolating material-specific performance differences.

During discharge, stored thermal energy is transferred through the HTF loop to the power conversion subsystem, represented by a simplified Rankine-cycle model. Electrical output is determined from:

$$P_{el} = \eta_{turbine}\eta_{generator}Q_{discharge} \quad (2.12)$$

where turbine and generator efficiencies are assumed constant to maintain controlled comparison across storage technologies.

System operation is governed by a supervisory control unit that regulates charging and discharge modes based on solar availability and storage temperature thresholds. The controller directs HTF flow, prevents discharge below operational limits, and maintains a daily operating cycle representative of decentralized solar electricity systems.

All subsystems are solved using a consistent variable-step numerical solver to ensure stability during transient conditions, particularly during PCM phase transitions. Energy transfer follows explicit pathways:

Charging mode:

Solar → Collector → HTF → TES

Discharge mode:

TES → HTF → Power block

This modular architecture improves subsystem transparency and enables reproducible evaluation of SHS and LHS technologies under identical climatic and operational conditions.

2.10 Numerical Implementation and Solver Configuration

The governing transient energy equations for sensible and latent storage systems were implemented in MATLAB/Simulink using interconnected dynamic function blocks.

Because phase-transition modeling in latent heat storage introduces numerical stiffness, simulations were performed using the variable-step implicit solver ode15s, which is appropriate for thermal systems with discontinuities in heat capacity.

The adopted solver settings were:

(i) Relative tolerance: 1×10^{-5}

(ii) Absolute tolerance: 1×10^{-6}

(iii) Maximum time step: 60 s

Adaptive time stepping was enabled to resolve rapid temperature variations during charging and phase transition periods. A time-step convergence test was conducted by reducing the maximum step size to 30 s, resulting in less than 1% variation in predicted stored energy, confirming numerical stability and solution convergence.

All simulations were performed over a 24-hour charge–discharge cycle under identical boundary conditions to enable consistent comparison between sensible and latent TES configurations.

3. Results and Discussion

3.1 Simulation Framework and Performance Indicators

Dynamic simulations were conducted to evaluate the thermodynamic performance of sensible and latent thermal energy storage (TES) systems integrated into a 100 kW solar electricity

generation system under the climatic conditions of North-Eastern Nigeria. A consistent 24-hour charge–discharge cycle was applied across all simulations.

Performance evaluation focused on the following indicators:

(i) Usable electrical-equivalent energy per cycle
(ii) Discharge stability
(iii) Round-trip thermal efficiency
(iv) Temperature evolution during charging and discharge

The analysis emphasizes comparative system behavior and its implications for dispatchable solar electricity generation.

3.2 Rock-Bed Sensible Heat Storage (SHS) Performance

The rock-bed sensible heat storage system exhibits the typical behavior of temperature-based thermal accumulation. During charging, solar heat transferred by the heat transfer fluid (HTF) progressively increases the temperature of the packed bed, reaching peak values close to 400 °C (Figure 2). The maximum recoverable thermal energy per cycle is approximately 210 kWh (Table 2), reflecting the inherent limitation of sensible storage, where energy density depends primarily on the temperature difference and specific heat capacity of the storage medium.

Table 2

Performance metrics of the rock-bed sensible heat storage (SHS) system.

Parameter	Value
Maximum temperature	~400 °C
Energy stored	~210 kWh
Efficiency	75–80 %
Power output	~95 kW decreasing to ~42 kW after 6 h

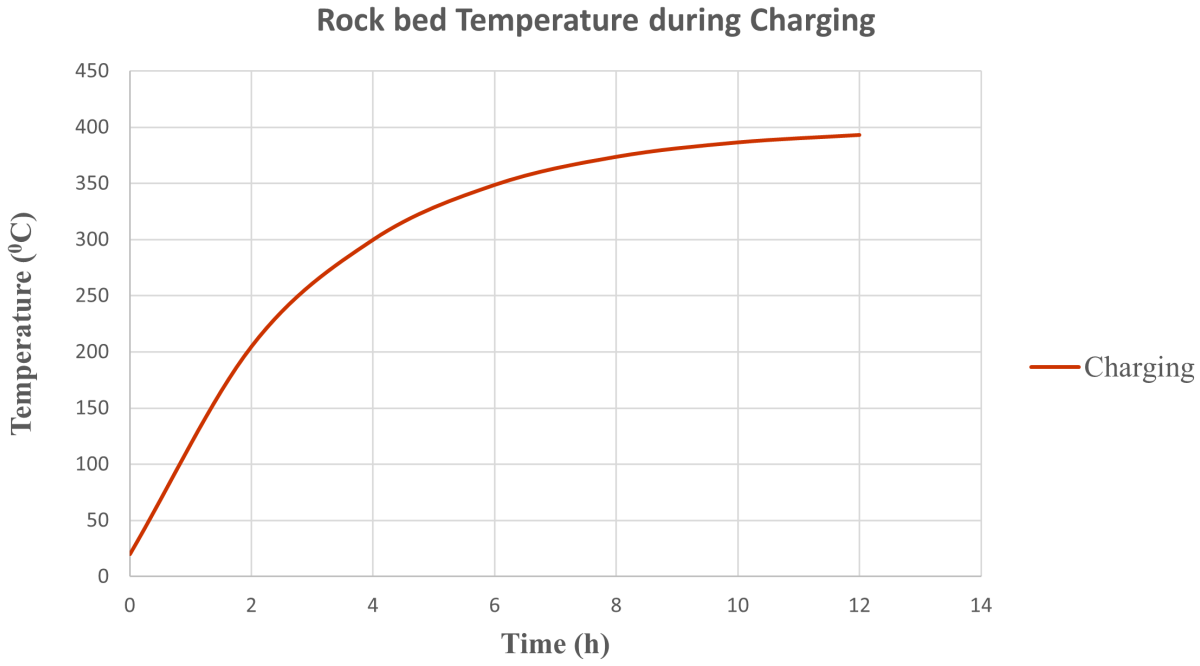

Figure 2

Temporal evolution of stored thermal energy in the rock-bed SHS system during a representative charging cycle.

During discharge, energy is released over an approximately six-hour generation period, with electrical output gradually declining as the temperature gradient between the storage medium and the HTF decreases (Figure 5). This behavior is typical of packed-bed systems where thermocline dispersion causes progressive mixing of hot and cold regions, leading to a steady reduction in power output despite relatively high round-trip thermal efficiencies of 75–80% (Figure 6).

Although the theoretical storage capacity of the rock bed, estimated from $Q = mC_p\Delta T$, is approximately 916 kWh, dynamic simulations indicate a recoverable energy of about 210 kWh per cycle. This difference results from operational constraints represented in the transient model. Heat storage occurs through thermocline propagation rather than uniform heating, meaning only part of the storage volume reaches the maximum temperature within the available charging period. In addition, limited daytime charging duration and heat transfer resistance between the HTF and solid medium further restrict energy uptake. Consequently, the effective storage utilization is approximately 23% of the theoretical capacity, consistent with observations reported for high-temperature packed-bed TES systems.

3.3 Latent Heat Storage (LHS) Systems: Material-Specific Behavior

Latent heat storage systems accumulate thermal energy primarily through solid–liquid phase transition, enabling near-isothermal heat absorption and release during operation. The daily storage behavior of the evaluated materials is illustrated in Figure 3, while key performance metrics are summarized in Table 3.

Table 3

Comparative performance of latent heat storage systems.

Storage Material	Max. Temp. (°C)	Energy stored (kWh)	Efficiency (%)	Power output (kW)
Solar Salt	~340	~1300	80–85	100 → 60
Sodium nitrate ($NaNO_3$)	~330	~780	78–82	100 → 52
Potassium nitrate (KNO_3)	~330	~520	77–81	100 → 46

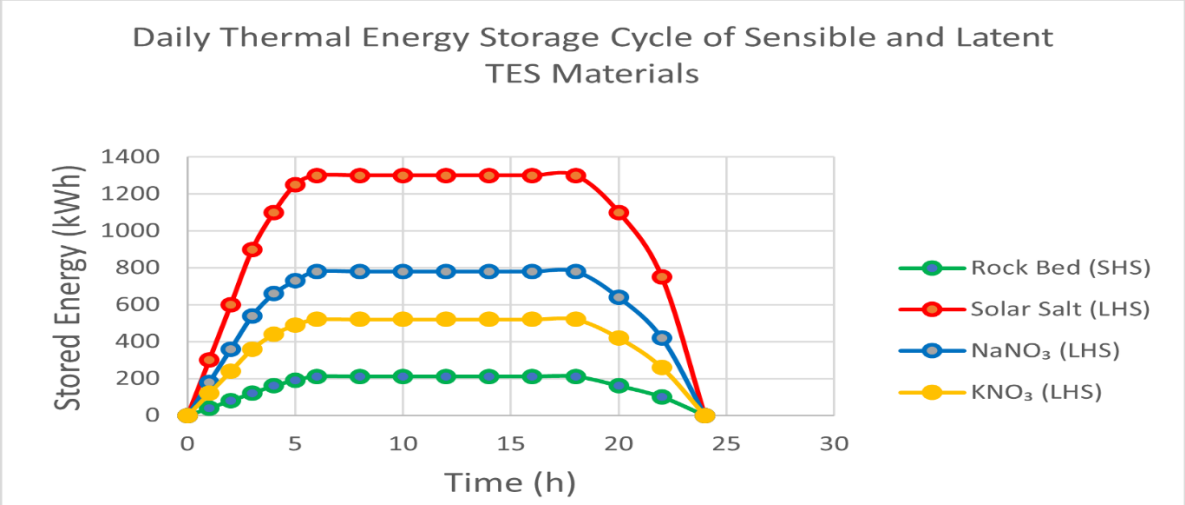

Figure 3

Daily TES operating cycle showing charging (0–6 h), storage hold (6–18 h), and discharge (18–24 h).

The 24-hour cycle consists of three stages: solar charging (0–6 h), thermal storage (6–18 h), and electricity generation during discharge (18–24 h). During charging, stored energy increases as solar heat is transferred to the storage medium, with the charging rate influenced by material thermophysical properties and heat transfer efficiency.

A clear difference exists between sensible and latent storage mechanisms. The rock-bed SHS system stores about 210 kWh, whereas latent heat storage systems achieve significantly higher capacities due to latent heat absorption during phase transition. Among the evaluated materials, Solar Salt shows the highest storage capacity (~1300 kWh per cycle), followed by sodium nitrate ($NaNO_3$) at ~780 kWh and potassium nitrate (KNO_3) at ~520 kWh under identical operating conditions. These differences highlight the thermodynamic advantage of phase-change materials, which combine sensible and latent heat storage.

During the 6–18 h storage period, the stored energy remains nearly constant, demonstrating the ability of TES systems to retain heat for delayed electricity generation beyond daylight hours. Solar Salt exhibits the most favorable thermodynamic behavior, achieving the highest round-trip efficiency (80–85%) and stable discharge performance. Sodium nitrate shows similar behavior with slightly lower efficiencies (78–82%), while potassium nitrate has the lowest storage capacity (~520 kWh), limiting discharge duration. The phase-change behavior responsible for these characteristics is illustrated in Figure 4 through the temperature evolution and phase-transition plateau of Solar Salt during charging.

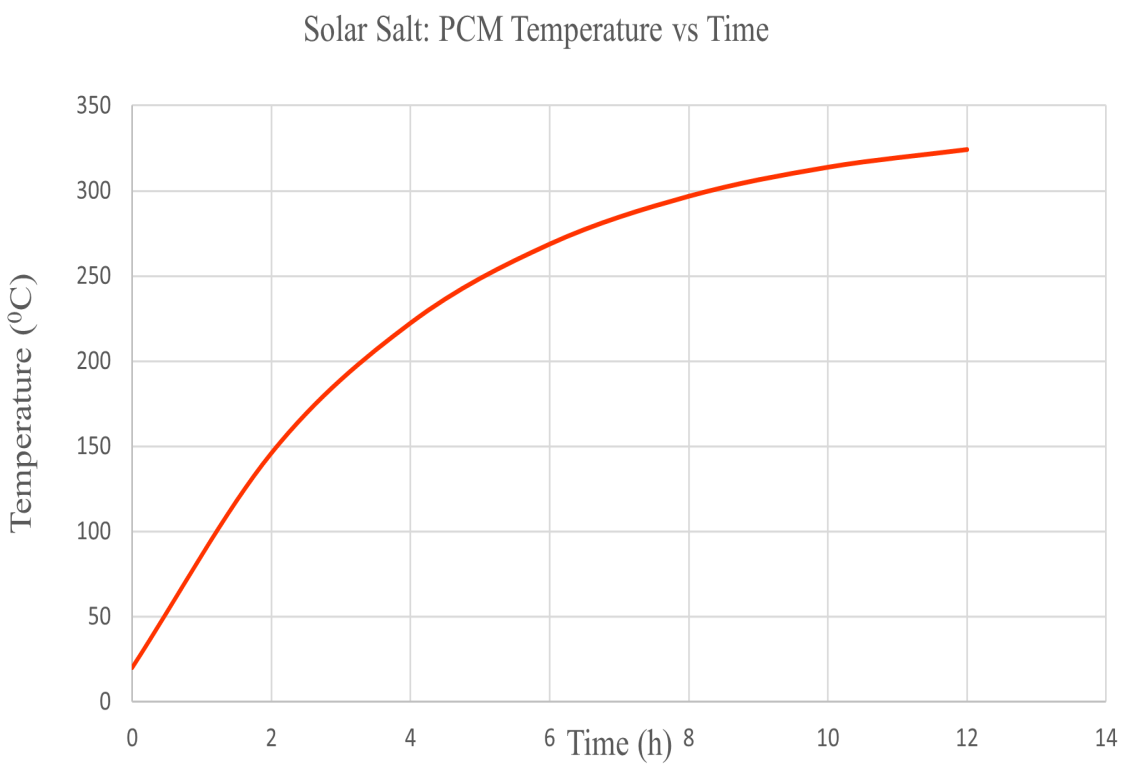

Figure 4

Temperature evolution of Solar Salt during charging, illustrating the phase-change plateau typical of latent heat storage.

3.4 Comparative System-Level Assessment

Discharge characteristics for all storage configurations are shown in Figure 5, while overall performance metrics are summarized in Table 4.

Table 4

Overall performance comparison of sensible and latent TES systems.

Parameter	Rock bed (SHS)	Solar salt (LHS)	Sodium nitrate (LHS)	Potassium nitrate (LHS)
Max. Temp (°C)	~400	~340	~330	~330
Energy stored (kWh)	~210	~1300	~780	~520
Efficiency (%)	75–80	80–85	78–82	77–81
Power output (kW)	95 → 42	100 → 60	100 → 52	100 → 46

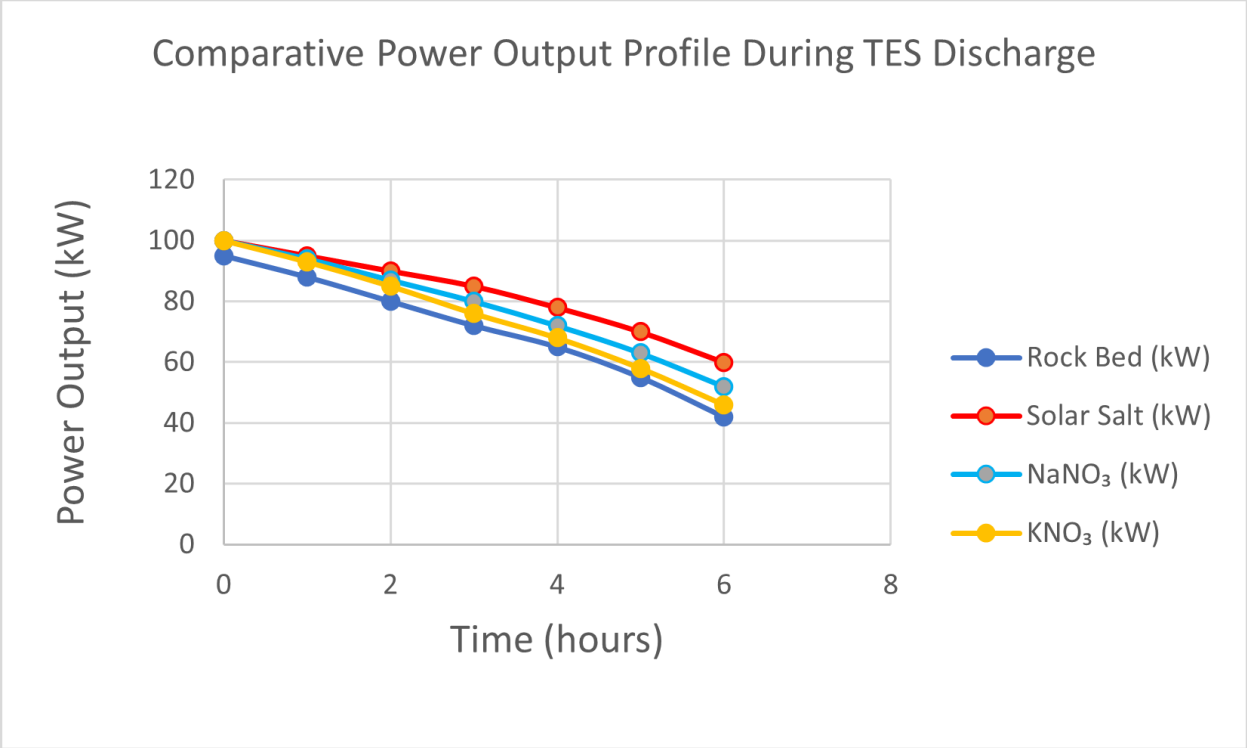

Figure 5

Power output profiles of TES systems during the discharge period.

Figure 5 illustrates discharge power profiles, highlighting differences in operational stability between sensible and latent storage systems. The rock-bed SHS system shows a continuous decline in output from approximately 95 kW to 42 kW, primarily due to thermocline dispersion and the gradual reduction in temperature gradient between the storage medium and the heat transfer fluid (HTF).

In contrast, latent heat storage systems exhibit smoother power profiles. The release of latent heat during solidification provides thermal buffering, enabling more stable heat transfer and power delivery during discharge. Among the evaluated materials, Solar Salt demonstrates the most stable output, decreasing from 100 kW to 60 kW. $NaNO_3$ and KNO_3 show similar behavior but with slightly larger declines, reaching approximately 52 kW and 46 kW, respectively.

Three main trends emerge from the comparison. First, latent heat storage offers significantly higher energy density, with Solar Salt storing roughly six times more energy than the rock-bed system under identical conditions (Figure 3). Second, latent systems provide improved discharge stability due to the phase-change buffering effect (Figure 5). Third, round-trip efficiencies are slightly higher for nitrate-based latent systems compared with sensible storage (Figure 6).

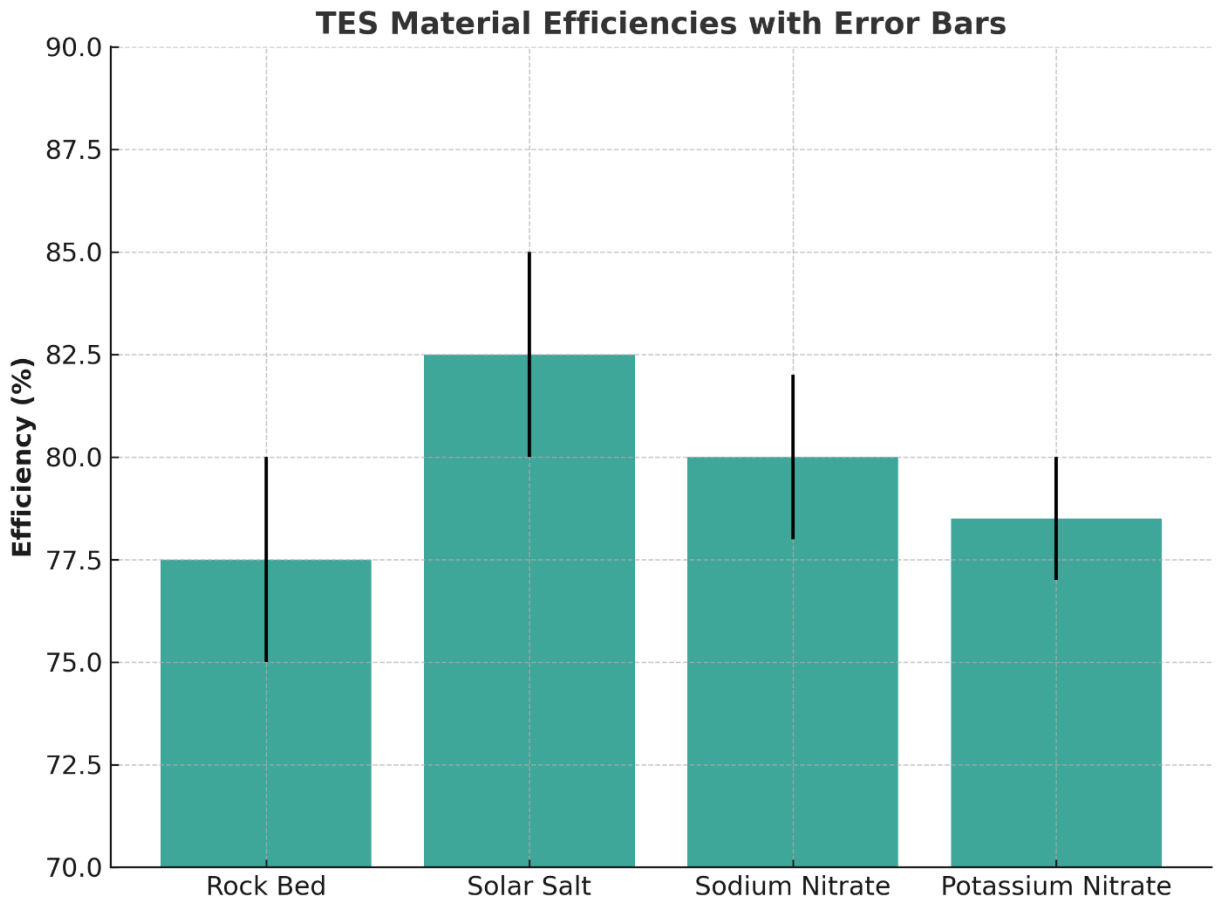

Figure 6

Comparative thermal efficiency of the rock-bed sensible heat storage system and latent heat storage systems using Solar Salt, $NaNO_3$, and KNO_3.

For dispatchable solar electricity generation, storage capacity and discharge stability are more critical than marginal efficiency differences. The results therefore highlight the operational advantages of nitrate-based latent heat storage, particularly in high-irradiance environments such as North-Eastern Nigeria.

3.5 Model Validation

The MATLAB/Simulink model was validated through comparison with published experimental and numerical TES studies operating under comparable temperature ranges. (Tian *et al*., 2022; Kumar *et al*., 2023; Abdelrahman *et al*., 2024). Validation considered round-trip efficiency, temperature evolution, and discharge stability. For the rock-bed SHS system, simulated round-trip efficiency ranged between 75–80%, consistent with reported experimental values of 70–82% for packed-bed TES systems operating between 250–400 °C. The model also reproduced characteristic thermocline propagation observed in experimental studies. For latent heat storage systems, simulated efficiencies were 80–85% for Solar Salt, 78–82% for $NaNO_3$, and 77–81% for KNO_3, which fall within reported performance ranges for nitrate-based TES systems. The model also reproduced the expected near-isothermal phase-transition plateau during charging and discharge.

Table 5

Model validation results comparing simulation predictions with literature values

Parameter	Simulation	Literature	Deviation
SHS round-trip efficiency	77%	75%	2.7%
LHS round-trip efficiency	83%	82%	1.2%
Thermocline behavior	Observed	Reported	Qualitative agreement

All deviations remain within ±5%, indicating good agreement with reported TES performance. Additional numerical convergence tests produced less than 1% variation in stored energy, confirming solver stability and reliability.

3.6 Implications for Solar Electricity Generation in North-Eastern Nigeria

The climatic conditions of North-Eastern Nigeria, characterized by high solar irradiance (~6 kWh m^{-2} day^{-1}), elevated ambient temperatures, and strong diurnal variability place specific demands on thermal energy storage systems intended for decentralized electricity generation.

In this environment, thermal energy storage technologies must satisfy several operational requirements:

(i) High volumetric energy density for medium-scale systems (~100 kW).
(ii) Stable discharge to support evening electricity demand.
(iii) Thermal robustness under elevated ambient conditions.
(iv) Consistent round-trip efficiency during daily cycling.

The simulation results indicate that nitrate-based latent heat storage systems outperform rock-bed sensible storage in terms of recoverable energy capacity and discharge stability under identical operating conditions. Solar Salt demonstrated the highest storage capacity (~1300 kWh), the longest quasi-stable discharge period, and the highest round-trip efficiency (80–85%). Sodium nitrate and potassium nitrate also exhibited reliable performance but with lower storage capacities. Although the rock-bed system showed predictable thermocline behavior and stable operation, its lower intrinsic energy density limited discharge duration at comparable system scale. These results suggest that latent heat storage particularly Solar Salt provides superior dispatchability for medium-scale solar electricity systems in arid high-irradiance regions.

3.7 Parametric Sensitivity Analysis

A parametric sensitivity analysis was conducted to evaluate the robustness of the simulation results. Key thermophysical and operational parameters were varied within realistic engineering ranges using a one-at-a-time (OAT) approach.

3.7.1 Sensible Heat Storage Sensitivity

Table 6.

Sensitivity of stored energy to variation in rock-bed specific heat capacity

Case	Cp Variation	Stored energy (kWh)	Deviation (%)
Baseline	0%	210	0
+10% Cp	+10%	231	+10
–10% Cp	–10%	189	–10

Results confirm the expected linear relationship between specific heat capacity and stored energy.

3.7.2 Latent Heat Storage Sensitivity

Latent heat of fusion was varied by ±10%.

Table 7.
Sensitivity of storage capacity to latent heat variation

Material	Baseline (kWh)	+10% L	–10% L
Solar Salt	1300	1430	1170
$NaNO_3$	780	858	702
KNO_3	520	572	468

Energy storage scales proportionally with latent heat magnitude, but the relative ranking of materials remains unchanged.

3.7.3 HTF Mass Flow Rate Sensitivity

HTF flow rate was varied by ±15%. Increased flow accelerated charging and extended stable discharge periods, while excessive flow slightly reduced thermocline sharpness in the SHS system. Latent systems demonstrated greater operational stability under flow variations.

3.7.4 Sensitivity Implications

Overall, the sensitivity analysis confirms that although absolute stored energy varies with thermophysical parameters, the comparative superiority of Solar Salt and latent heat storage remains consistent.

4. Conclusions

This study developed a unified MATLAB/Simulink simulation framework to compare rock-bed sensible heat storage (SHS) and nitrate-based latent heat storage (LHS) systems for a decentralized 100 kW solar electricity configuration representative of North-Eastern Nigeria. Using identical climatic inputs and operational conditions, the framework enabled consistent evaluation of storage technologies based on energy capacity, discharge stability, thermocline behavior, and round-trip thermal efficiency. Results show that latent heat storage systems significantly outperform the rock-bed SHS system in usable energy capacity. The SHS configuration stored approximately 210 kWh per cycle and exhibited a gradual decline in power output during discharge due to thermocline dispersion. In contrast, nitrate-based PCMs achieved substantially higher storage capacities. Solar Salt demonstrated the best overall performance, with about 1300 kWh storage capacity per cycle, stable quasi-isothermal discharge, and round-trip efficiencies of 80–85%. Sodium nitrate ($NaNO_3$) and potassium nitrate (KNO_3) also showed reliable operation but with lower storage capacities. Sensitivity analysis indicated that variations in thermophysical properties and heat transfer fluid flow rate affect the magnitude of stored energy but do not change the relative performance ranking of the materials. Numerical convergence tests further confirmed the stability of the simulation framework. Overall, the results highlight the advantages of nitrate-based latent heat storage for improving the dispatchability of solar electricity systems in high-irradiance regions. In particular, Solar Salt shows strong potential for decentralized solar power systems in North-Eastern Nigeria where reliable electricity supply is limited. Future studies should focus on experimental validation and techno-economic assessment of TES integration in decentralized solar energy systems.

References

Abdelrahman, A., Wang, Y., & Li, Q. (2024). Experimental and numerical investigation of nitrate-salt-based latent heat storage for concentrated solar power. *Applied Thermal Engineering, 250*, 118760. https://doi.org/10.1016/j.applthermaleng.2023.118760

Cabeza, L. F., de Gracia, A., & Fernández, A. I. (2021). Advances in thermal energy storage materials and systems: A critical review. *Renewable and Sustainable Energy Reviews, 141*, 110123. https://doi.org/10.1016/j.rser.2021.110123

European Commission Joint Research Centre (JRC). (2023). *Solar resource maps of Africa*. https://re.jrc.ec.europa.eu

International Energy Agency (IEA). (2023). *Energy storage: Tracking clean energy progress*. https://www.iea.org

International Renewable Energy Agency (IRENA). (2022). *Innovation outlook: Thermal energy storage*. https://www.irena.org

Kumar, P., Singh, R., & Sharma, A. (2023). Numerical study of nitrate-based latent heat storage for concentrated solar power plants. *Energy Conversion and Management, 287*, 116637. https://doi.org/10.1016/j.enconman.2023.116637

Li, G., Wang, X., & Li, Y. (2023). Numerical investigation of packed-bed sensible heat thermal energy storage for solar thermal systems. *Energy, 263*, 125137. https://doi.org/10.1016/j.energy.2022.125137

National Aeronautics and Space Administration (NASA). (2023). *NASA POWER: Surface meteorology and solar energy data*. https://power.larc.nasa.gov

Peng, S., Li, P., & Ding, J. (2020). Performance analysis of rock-bed thermal energy storage for solar power applications. *Energy Conversion and Management, 205*, 112118. https://doi.org/10.1016/j.enconman.2019.112118

Prieto, C., Rodríguez, A., Cabeza, L. F., & Martorell, I. (2022). State of the art of molten salts as thermal energy storage materials in concentrating solar power plants. *Solar Energy, 231*, 256–274. https://doi.org/10.1016/j.solener.2021.11.031

Tian, Z., Liu, H., & Yang, X. (2022). Dynamic simulation of packed-bed TES systems under daily solar cycles. *Applied Energy, 308*, 118293. https://doi.org/10.1016/j.apenergy.2022.118293

World Bank. (2020). *Access to electricity (% of population) – Nigeria*. World Bank Open Data. https://data.worldbank.org

Xu, B., Li, P., & Chan, C. L. (2020). Application of phase change materials for thermal energy storage in concentrated solar thermal power plants: A review. *Applied Energy, 259*, 114152. https://doi.org/10.1016/j.apenergy.2019.114152

Zhang, Y., Wang, R., & Li, X. (2021). Thermal performance evaluation of nitrate-based phase change materials for high-temperature energy storage. *Journal of Energy Storage, 41*, 102118. https://doi.org/10.1016/j.est.2021.102118